Computer Simulation of Discrete Crack Propagation

Ioannis Mastorakos, Lazaros K. Gallos
Laboratory of Mechanics and Materials, Polytechnic School,
Aristotle University of Thessaloniki, GR-54006 Thessaloniki, Hellas
Elias C. Aifantis
Laboratory of Mechanics and Materials, Polytechnic School,
Aristotle University of Thessaloniki, GR-54006 Thessaloniki, Hellas
and
Center for Mechanics of Materials, Michigan Technological University,
Houghton MI 49931, USA

ABSTRACT

Although statistical methods are widely used to study a large amount of phenomena ranging from random walk to percolation and particle charging, the application of these methods to mechanics is limited. Nevertheless the use of senses like fractal dimension can be very handy to describe the "mass" of a crack or the roughness of a surface.

From this viewpoint subcritical crack growth is studied as a cluster growth process with the aid of discrete "computer experiments". A mechanical ballistic aggregation model motivated by a continuum theory of stress-assisted migration of point defects is formulated and simulated on a square lattice. These defects move towards the crack tip under the action of the high stress gradients existing there. The crack grows by the "influx" of defects in the tip region with the rate of this process, which depends on the externally applied stress, determining the crack velocity and its dependence on the stress intensity factor. The crucial parameter of the model is the initial concentration of defect particles. It is shown that there is a characteristic relation between critical stress and crack growth for different initial defect concentrations. The crack path is of a fractal character and the crack velocity dependence on the stress intensity factor follows a power law relationship, in accordance with experimental trends.

I. INTRODUCTION

Subcritical cracking /1, 2/ is a generic term used to indicate slow crack growth for applied loads below those causing dynamic fracture. Subcritical cracking may occur under creep, fatigue, hydrogen embrittlement

9

and stress corrosion cracking conditions. In all these cases the evolution of microstructure near the crack tip is such that it promotes bond breaking or other microfracturing processes which are directly responsible for crack propagation. For example, in the case of hydrogen embrittlement, atomic hydrogen is diffusing in the crack tip region under the influence of high stress gradients that are present there for nominal applied loads. The high hydrogen concentration promotes bond breaking (lattice decohesion) or dislocation emission (lattice softening to dislocation motion) and both of these mechanisms cause slow crack growth. Current research in fracture mechanics /3-7/ concentrates on dynamic crack propagation, including the question of terminal crack velocities in bulk as compared to Rayleigh wave speed in homogeneous bulk materials /7/, as well as to supersonic crack velocities in bimaterial interfaces /8/. Additionally, current work focuses on the problem of crack morphology including the zig-zag nature of the crack path /4, 9/. In contrast, the problem of slow crack propagation or subcritical crack growth has not attracted similar attention in the mechanics literature, even though it has been a long-standing issue in the materials science literature. In fact, there is a variety of interesting non-linear effects associated with subcritical cracking, including non-convex fracture resistance vs. crack velocity curves and stick-slip fracturing (see, for example, /1, 10/ and references quoted therein). Both of the aforementioned dynamic fracture problems of crack velocity estimation and crack morphology determination become even more important in the case of subcritical cracking which is one of the central mechanisms for component failure. In this connection, it is emphasized that among the central open questions in subcritical cracking are those concerned with predicting crack shape and morphology, as well as the crack-tip velocity of propagation and its dependence on external load or applied stress intensity factor. Eventually, it is expected that the rich variety of crack morphologies seen in experiments and in nature will be connected to the dominant mechanisms of crack growth. In addition, determination of crack velocity would become possible as part of the problem solution, rather than imposing it a priori as is the case in a plethora of previous published elastodynamic or pseudoplastic analyses of crack propagation.

In contrast to the mechanics and (in part) the material science literature, considerable activity has been devoted recently in the physics literature to understanding the problem of crack velocities and morphologies via computer simulations of spring networks /11/ with local bond breaking criteria dependent on the prevailing stress (and/or its gradient) level. In particular, fracture processes in disordered media are studied with the focus on crack morphologies by using fractal geometry /12/. Although simple in concept, such simulations pose a great challenge due to the very large super-computing resources required /11/. Another line of research, using discrete "cluster growth" models, has also provided valuable insight into the connection between microscopic growth mechanisms and resulting macroscopic patterns in a variety of aggregation/deposition phenomena (see, for example, /12/ for a review).

The modest goal of the present paper is to outline a combined phenomenological computer simulation model to study subcritical crack growth as a cluster growth process. In particular, a mechanical ballistic aggregation model motivated by a continuum stress-assisted migration of point defects is formulated and simulated on a lattice. The crack grows by the flux of defects to the tip region due to the high local stress gradients existing there as a result of the elastic singularity. The accumulation of defects may cause either

10

continuous extension of the crack tip (due, for example to vacancy absorption) or discontinuous crack growth by the formation of microcracks ahead of the main crack (due, for example, to creep damage or hydrogen embrittlement) and subsequent propagation to join the advancing tip. The crucial parameters for the model are the initial concentration of defect particles and the stress which defines the force for a "particle" to move to the growing crack. The crack path is of a fractal character and the crack velocity dependence on the stress intensity factor follows a power law relationship, in accordance with experimental trends.

As mentioned in the previous paragraphs, the basic physical assumption made in the present work is that the motion of defects to the crack tip is the limiting process controlling crack growth. It is further assumed that this motion and/or accumulation is directly governed by the high stress gradients existing at the crack tip. Depending on the particular fracture mechanism that takes place in the near-tip region, the defects may be identified as vacancies (high-temperature creep), microvoids (damage), dislocations (plasticity) or hydrogen atoms (hydrogen embrittlement). The phenomenological assumption common to all these mechanisms is that the defects or their clusters are driven towards the crack tip region by the high stress gradient set up there by the elastic singularity induced by the applied loads. Justification for this assumption can be found in the literature for all cases: see, for example /13/ for the case of vacancies and microvoids, /14/ for the case of dislocation dipoles and /15, 16/ for the case of hydrogen embrittlement. To illustrate the basic ideas and the phenomenology involved, we consider in the next section, Section 2, the case of hydrogen embrittlement and derive a power-law relation for the crack velocity vs. stress intensity factor based on a chemical-like fracture criterion. The limitations of such purely phenomenological derivation thus become apparent, since it is strongly dependent on the specific details of the stress-assisted migration model assumed and provides no information on the crack morphology and fractal nature of the crack path. These limitations are removed by the discretization scheme introduced in Section 3, where an initial crack is embedded in a lattice with a portion of its cells occupied by the migrating defects. The migration of defects is governed by transition probabilities which are expressed in terms of the appropriate stress gradient components derived from elastic fracture mechanics. Based on this, computer simulations are performed. The results, reported in Section 4, establish a power law relation between crack velocities and stress-intensity factors. Finally, a discussion of these results is presented in Section 5.

2. THE CASE OF HYDROGEN EMBRITTLEMENT

Hydrogen Embrittlement is a generic term describing a wide variety of fracture phenomena involving hydrogen. Hydrogen may be either internal as a result of melting and casting practices or external due to the pickling, electroplating on cathodic process. Of all interstitial elements, hydrogen migrates fastest in metals and alloys, particularly in iron and steel. Hydrogen transport in dislocation cores or in the form of associated Cottrell atmosphere may be several orders of magnitude faster than lattice diffusion. Hydrogen trapping occurs at various depths and is associated with a wide variety of locations in the microstructure including

solutes and dislocations, grain boundaries, inclusions, precipitates and voids. Embrittlement occurs in a wide range of materials. It is particularly important for steels, and also for high strength nickel-base alloys, titanium alloys and materials used in the nuclear power industry (zirconium, hafnium, niobium, uranium). Most hydrogen embrittlement fractures are intergranular, but cleavage-like cracking can also occur, especially if transgranular brittle hydrides form and act as crack nucleation sites. Besides hydride formation in the material, hydrogen can remain in the lattice and interact with dislocations and other lattice defects. When hydrogen originates in the bulk (internal embrittlement), hydrogen transport is a simple process and is most often controlled by the lattice diffusion process which takes place by the movement of a screened proton that has given up its electron to the electron gas of the metal. When hydrogen originates externally (external embrittlement), it is required to absorb on an external surface, chemisorb, and enter the metal lattice as a screened proton. A simple chemomechanical model which seems to be equally valid for both internal and external embrittlement, has been proposed by Aifantis /16/ and subsequently elaborated upon by Aifantis and co-workers /17-19/ (see also a recent book by Unger /20/). Central to this phenomenological model is the assumption that cracking is controlled by the level of concentration of embrittling hydrogen species at a critical distance ahead of the crack tip. The critical distance can usually be identified to the grain or plastic-zone size and, in the absence of a predominant microstructure, may shrink to zero by assuming it to asymptotically approach the crack tip. The material confined by the critical distance in the neighborhood of the crack tip is highly inelastic and no attempt is made to model its chemomechanical response. The material further away is governed by a simple concentration-dependent linear elastic constitutive equation. The differential equation describing the spatial and temporal distribution of the hydrogen species in the presence of a hydrostatic stress field σ_h reads

$$\dot{\rho} = (D + N\sigma_h)\nabla^2\rho - (M - N)\nabla\sigma_h\nabla\rho \tag{1}$$

where ρ denotes concentration and the chemomechanical coefficients D, M and N are assumed to be constants. This stress-assisted diffusion equation was derived by Aifantis /15, 21/ in an effort to model solute transport in stressed solids. It is a consequence of the standard differential equation expressing the conservation of mass for the diffusing species $\dot{\rho} + \nabla\rho = 0$ and the following modification of Fick's law of diffusion ,

$$\mathbf{j} = (D + N\sigma_h)\nabla\rho + M\nabla\sigma_h \tag{2}$$

where $\mathbf{j}$ denotes the flux of the diffusing species, while the hydrostatic stress field σ_h is harmonic ($\nabla^2\sigma_h = 0$) for elastic deformations. The zero flux steady-state solution of Eq. (1) or equilibrium solution of Eq. (2) reads,

12

$$\rho = \rho_0 (1 + \beta \sigma_h)^a \tag{3}$$

where ρ_0 is the concentration on the boundary and $\alpha = M/N$, $\beta = N/D$ are new phenomenological constants. Strictly speaking, the relationship given by Eq. (3) is valid for points which lie outside a small region surrounding the crack tip and defined by a "critical distance" determined by the particular constitutive structure of the material. For perfectly elastic materials this "critical distance" approaches zero. Next, we express Eq. (3) in terms of the stress intensity factor. For the usual Mode I crack problem (opening mode), elasticity theory derives the following singular expression for the hydrostatic stress,

$$\sigma_h = \frac{K_I}{\sqrt{2\pi r}} \cos\left(\frac{\vartheta}{2}\right) \tag{4}$$

(where (r, ϑ) denote the polar coordinates with the crack tip considered in the origin, $K_I = 1.12\sigma_\infty \sqrt{2\pi\alpha}$ is the stress intensity factor for a crack located in one edge of the sample, σ_∞ denotes the tensile stress at infinity and α is the crack length). For loading states for which the stress intensity factor K_I varies slowly above the critical stress intensity factor K_I^c, the phenomenological model assumes /16/ that the crack velocity v can be expressed as a power series of the value of the concentration ρ at a critical point (r_c, ϑ_c) ahead of the crack tip, i.e.

$$v = \sum_{m=0}^{n} c_m \rho^m$$

where c_m are constants and n is the order of the last term in a truncated series. Upon substituting Eq. (4) into Eq. (5) and evaluating it at (r_c, ϑ_c) for two different pairs of velocities and stress intensity factors (v_1, K_{I1}) and, (v_2, K_{I2}) one obtains /16/ the power law relation

$$v = v_0 K_I^d \tag{6}$$

when the critical distance approaches asymptotically the crack tip ($r_c \to 0$), or the relation

$$v = \overline{v}_0 (1 + \gamma K_I)^d \tag{7}$$

when the critical distance r_c is assumed to be a material parameter; say equal to a grain size for a polycrystal. The quantities v_0 and $\overline{v}_0$ denote reference values of the crack velocity in the respective v vs. K_I graph. The exponent d is given by $d = n\, M / N$ while the constant γ is given by $\gamma = NAD / \sqrt{r_c}$. Relations (6) and (7) do not hold near the critical stress intensity factor K_I^c where the crack velocity "jumps" from zero to finite values.

13

3. THE MODEL

In this section we describe the computational model that we used for simulating crack propagation due to hydrogen embrittlement.

We consider a two-dimensional sample under external stress (Figure 1). The sample is discretized and the lattice so formed contains sites, which can be in one of the following three states: a) solid (part of the sample bulk), b) defect site (due to the presence of hydrogen), and c) crack site (part of the crack). The lattice size is $5LxL$, where we assumed values of L in the range 500-1000, with a lattice constant equal to 100 nm. A seed cell is placed at $(0,L/2)$ representing the crack tip. Hydrogens are randomly distributed in the sample with a concentration ρ of the total number of sites, thus giving rise to a random distribution of defect sites. These hydrogens move due to the stress field imposed by the presence of the crack tip. An external stress $\sigma_\infty=1$ GPa is applied (the value of the stress, in fact, influences only the time-scale of the problem and not the general behavior of the system). A hydrogen bath exists in the side opposite to the initial crack tip. Whenever a defect comes to within a lattice unit from the existing crack, it becomes irreversibly part of it, and the crack propagates. The simulation algorithm is as follows:

i) The stress field is assumed to be given by the classical elasticity solution; in particular its asymptotic form near the crack tip. We have considered Mode I plane stress conditions, as described in Eq. (4). It can be shown by calculating the gradient of σ_h in polar coordinates that the migration velocities of hydrogens in the sample are given by:

$$v_x \sim r^{-3/2} \cos\left(\frac{\theta}{2}\right)(1 - 2\cos\theta) \qquad v_y \sim r^{-3/2} \sin\left(\frac{\theta}{2}\right)(1 + 2\cos\theta) \qquad (8)$$

At each time step, we compute the velocities for all hydrogens in the sample from the above equations.

ii) The magnitude of the velocity $|v|$ for each defect site is then calculated and the time δt needed for the hydrogen to cover a distance equal to the lattice constant is sampled from an exponential distribution based on this velocity, i.e. $\delta t = - \ln(R)\, \alpha \,/\, |v|$, where R is a uniformly distributed random number, and α is the lattice constant.

iii) The defect with the shortest time δt_{min} is allowed to move towards the crack tip and the overall time increases by the same amount.

iv) The direction towards where the motion takes place is determined by the weighted local transition probabilities $P_x=v_x/(v_x+v_y)$ and $P_y=v_y/(v_x+v_y)$.

v) If the defect comes to a site which is neighbor to the crack, it irreversibly becomes part of the crack itself. A new defect site is created inside the hydrogen bath in order to ensure constant hydrogen concentration throughout the sample. A check is performed in order to identify whether the new crack site is further from the origin than the current crack tip. If this is the case, the crack tip is considered to lie on this new site and all the subsequent calculations are repeated according to this crack tip.

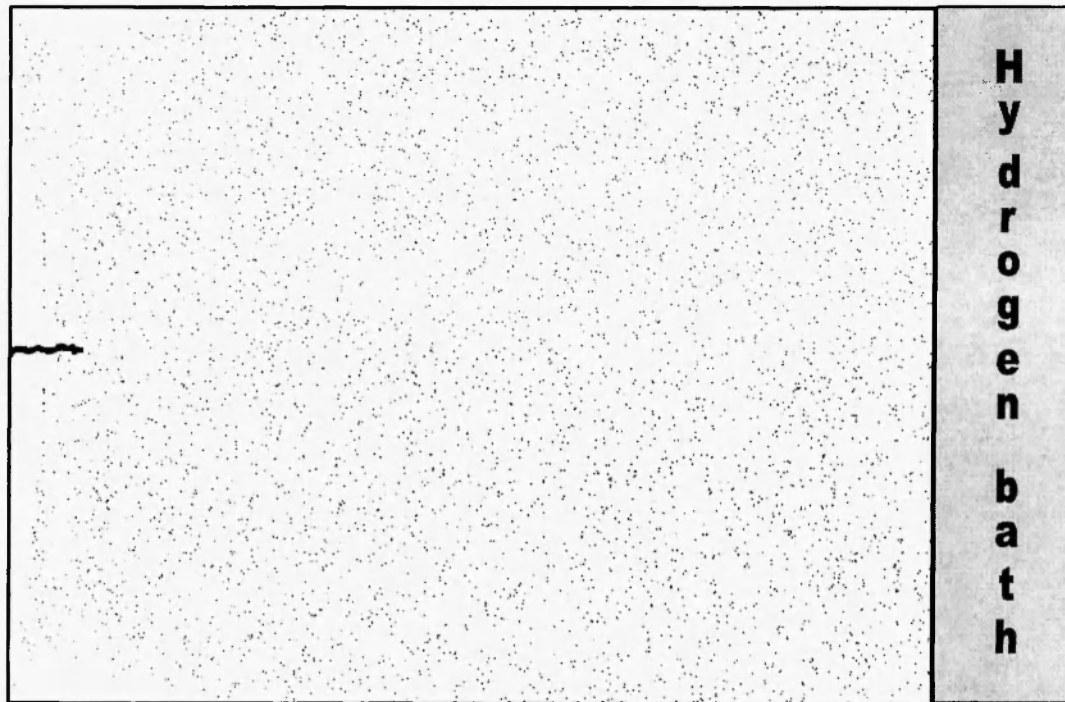vi) The above procedure is repeated from step i) until a predefined time interval has elapsed.

Fig. 1: Schematic representation of the model. The thick line represents the crack, dots denote the local hydrogen concentration and we can also see the attached hydrogen bath.

4. RESULTS

Examples of cracks generated with the described simulation procedure for different hydrogen concentrations are shown in Figure 2. We can see that, in general, the model gives rise to many different pattern formations, mainly of stochastic nature, which propagate in the sample. There is also the probability of deviating from parallel to the edge propagation, with cracks moving diagonally in a local scale. This phenomenon is attributed mainly to the local hydrogen concentration that creates "paths" which can be traced more easily in the sample. This is mainly the case for high concentrations. On the contrary, a well-defined linear propagation with small fluctuations is observed at low concentrations. These trends will be discussed later.

In Figure 3 we present a plot of a typical tip displacement as a function of the time. The crack propagates in steps, rather than continuously, as can be seen in the inset of the figure, and this ladder-type curve has also been experimentally observed /4,9/. The slope of the curve provides an estimate for the crack tip velocity, but, as can be seen in the plot, the slope is not constant throughout the simulation, meaning that the tip velocity is also time-dependent.
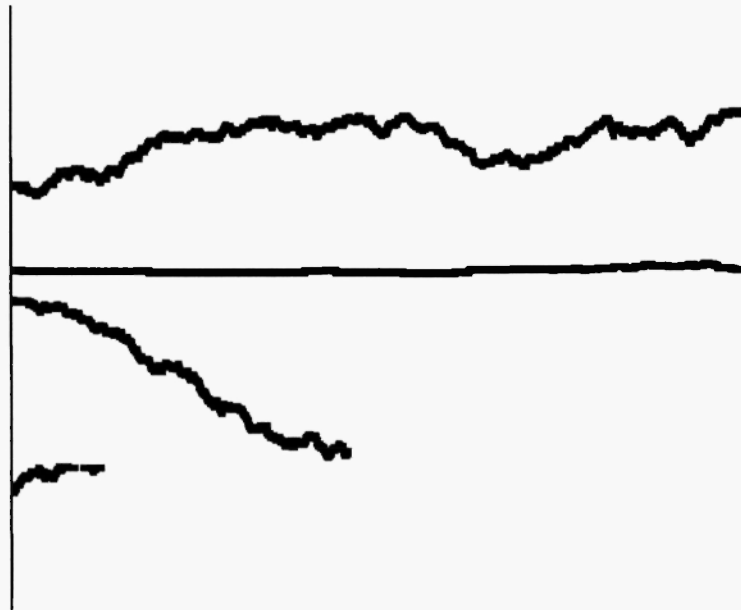
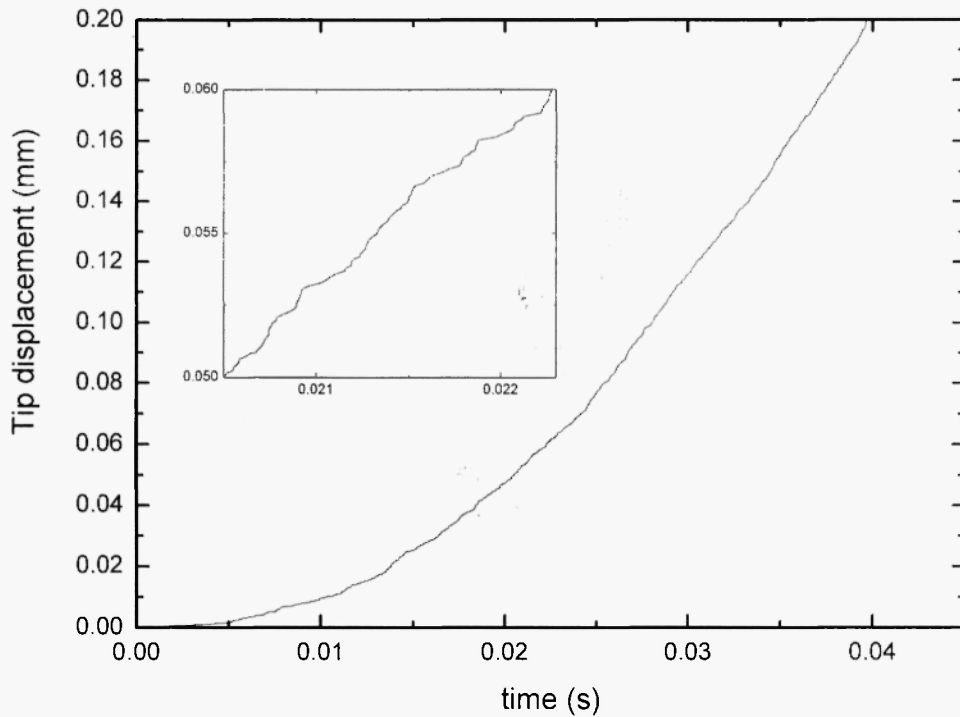**Fig. 2:** Different crack morphologies, as derived by different realizations of the simulation.

Fig. 3: Typical evolution of the crack tip displacement as a function of time. The inset is a magnification of the curve showing a quite discontinuous propagation.

16

Thus, averaging over finite time intervals, we can construct a plot of the crack tip propagation velocity as a function of time. This is presented in Figure 4, where we display the results for a number of different hydrogen concentrations. At higher concentrations the tip velocity increases with time in a roughly constant rate (ignoring the statistical fluctuations due to the averaging and the finite sample size). At low concentrations a very different picture emerges with a practically constant velocity at early times, which is followed by a dramatic increase in a very short time interval. Notice also the different time scales needed for the crack to propagate under different concentrations; while only a fraction of the second is required for high ρ, propagation at the same distance for low ρ may need some minutes.
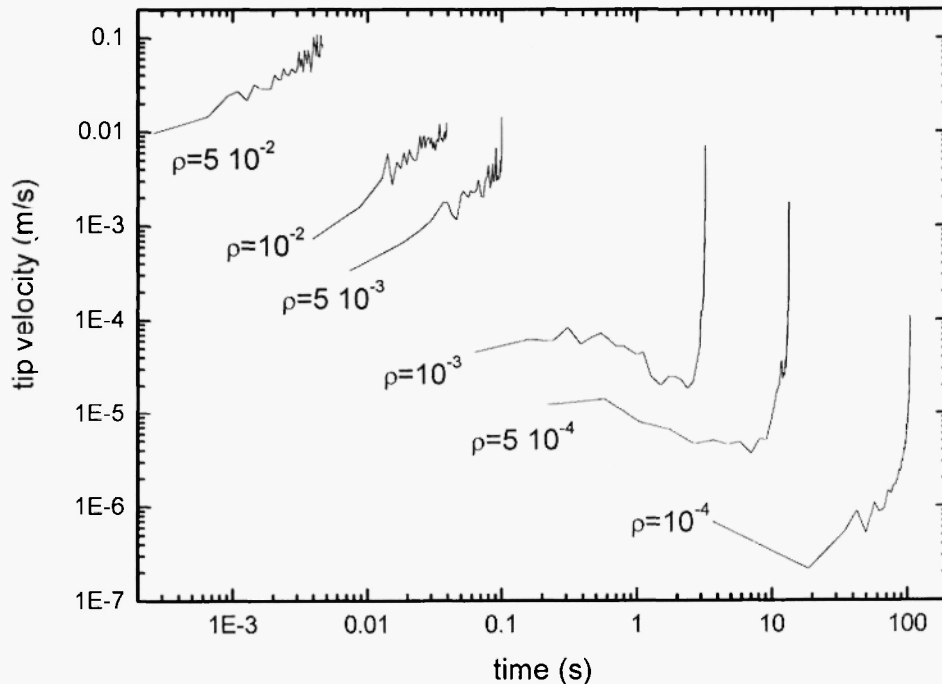

Fig. 4: Crack tip velocity, averaged over 100 realizations, for different hydrogen concentrations ρ, as a function of time.

During the simulation, we can compute the stress intensity factor K_I, which is modified due to the varying crack length, so that we can plot the crack tip velocity as a function of K_I, as shown in Figure 5. The curves present a similar behavior to those in figure 4, with higher concentrations yielding roughly a power law, and lower concentration curves being initially parallel to the x-axis followed by an abrupt increase. The relative velocities are also markedly different, with two to three orders of magnitude higher propagation rates for higher ρ at a given K_I.
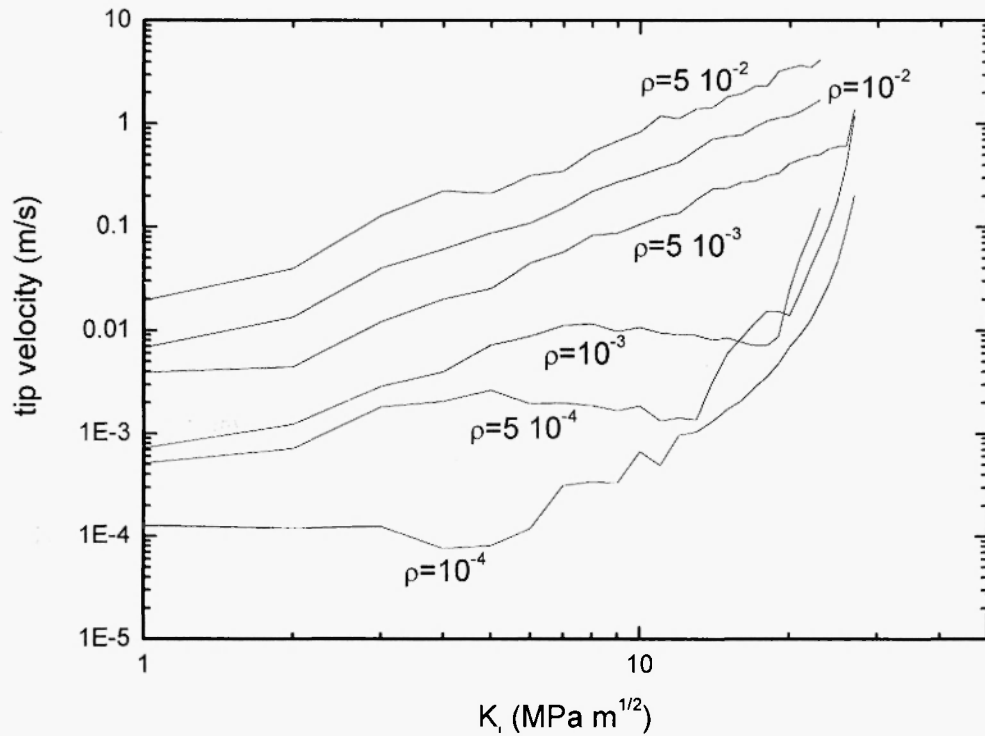
17

Fig. 5: Crack tip velocity as a function of the stress intensity factor for different hydrogen concentrations.

From Figure 5 we can compute the slopes of the relation $v_{tip} \sim K^n$. For the low-ρ curves, which do not follow this law for the whole K_I range, we only use the asymptotic regime. The exponent n versus the hydrogen concentration is displayed in Figure 6. It is clear that for high ρ the rate is constant and the slope is equal to roughly 1.9, while a transition regime is observed with the exponents taking the value of 14 at lower concentrations.

5. DISCUSSION

In this work we used a simple computational model for the study of crack propagation by taking into account known analytical formulas for the stress field created by the crack. Hydrogens move in this field with a stochastic element in their motion, and when they attach themselves on the existing crack, they force it to propagate further.

With this model we were able to observe different crack morphologies, from very rough to almost linear cracks, with the main factor being the hydrogen concentration in the sample. The tip propagation velocity, also, is a strong function of the hydrogen concentration ρ. Moreover, a very different behavior was exhibited for the tip velocity as a function of K_I at different ρ.
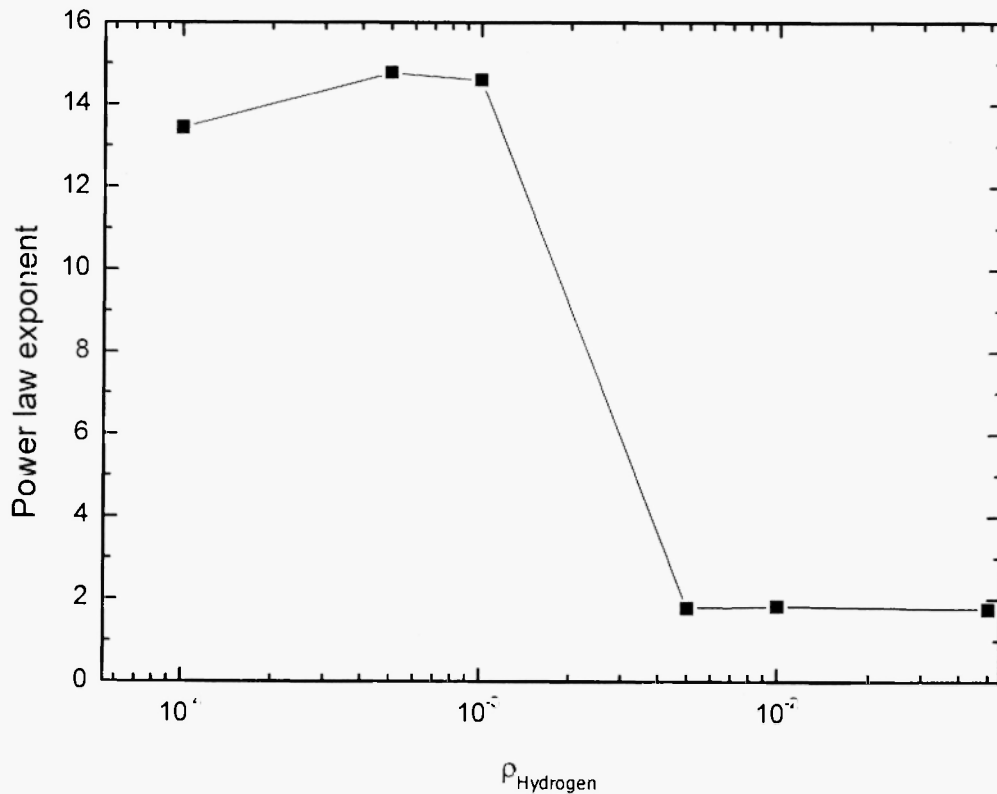
18

Fig. 6: Dependence of the power law exponent, as derived by the curves in figure 5, on the hydrogen concentration. Note the sharp transition in the behavior of the exponent.

Our explanation on this strong ρ dependence is as follows. When the hydrogen concentration is high enough, the local environment around the tip is the same at practically all times. The tip cannot attract all the hydrogen in its neighborhood, so it propagates in a constant rate. The shape of the crack is determined by local hydrogen concentration fluctuations, and the crack follows a path, in analogy to the invasion percolation model /22/. Of course, the higher the concentration the faster is the velocity of the crack tip, as observed in the simulations, too.

At low hydrogen concentrations, though, all the hydrogen of the sample is rapidly consumed, since it is strongly attracted by the tip. This creates a depletion zone and after this initial stage there is no hydrogen in the sample to assist the crack propagation. However, the hydrogens provided by the bath now become the principal motive force for the crack evolution. At first, the attraction is not large enough, but as the crack length increases, the field becomes progressively stronger, resulting in the rapid increase of the hydrogen attachment to the crack. This also explains the straight-line form of the crack at low-ρ: hydrogens departing from the bath quickly converge to a line extending in front of the crack and then follow a straight path towards the tip.

Of course, the exact results depend on the placement of the bath, since a bath at longer distances or to a different position will yield a quantitatively different outcome. However, the main qualitative picture will remain the same, with different behavior mainly at low-ρ, since at high-ρ situations it is the local environment which is important, and the results are largely independent of the presence of a bath.

REFERENCES

1. T. Webb and E.C. Aifantis, Stick-slip peeling, ASME winter annual meeting, San Francisco, CA, No. 89-WA/EEP-47 (1989) .

2. D.A. Meyn, Effect of hydrogen content on inert environment sustained load crack propagation mechanisms of Ti-6Al-4V, In: *Environmental Degradation of Engineering Materials*, M.R. Louthan Jr. et al. (Eds.), Virginia Tech Printing, Blacksburg, VA, 1981; 383-392.

3. H. Gao, A theory of local limiting speed in dynamic fracture, *J. Mech. Phys. Solids* **44** (9), 1453-1474 (1996).

4. M. Marder, New dynamical equations for cracks, *Phys. Rev. Lett.* **66**, 2484-2487 (1991).

5. J. Lambros and A. Rosakis, Development of a dynamic decohesion criterion for subsonic fracture of the interface between two dissimilar materials, *Proc. R. Soc. Lond. A*, **1995**, 711-736.

6. J. Rice, Y. Ben-Zion and K.S. Kim, Three dimensional perturbative solution for a dynamic planar crack moving unsteadily in a model elastic solid, *J. Mech Phys. Solids* **42**, 813-843 (1994).

7. L.B. Freund, *Dynamic Fracture Mechanics*, Cambridge University Press, New York, 1990.

8. J. Lambros and A. Rosakis, Shear dominated transonic interfacial crack growth in a bimaterial - 1. Experimantal observations, *J. Mech. Phys. Solids* **41** (3), 457-486 (1995).

9. H. Gao, Surface roughening and branching instabilities in dynamic fracture, *J. Mech. Phys. Solids* **41**, 457-486 (1993).

10. T. Webb, On the theory of stick slip fracture, PhD Dissertation, MTU, Houghton, 1993.

11. H. Herrmann and S. Roux, *Statistical Models for the Fracture of Disordered Media*, North-Holland, Amsterdam, Netherlands, 1990.

12. B.B. Mandelbrot, *The Fractal Geometry of Nature*, Freeman, New York, 1983.

13. J. Collios and E.C. Aifantis, On the problem of a continuum theory of embrittlement, *Res Mech.* **5**, 67-85 (1982).

14. J. Kratochvil, Continuum mechanics approach to collective behavior of dislocations, *Solid State Phenomena* **35-36**, 71-86 (1994).

15. E.C. Aifantis, On the problem of diffusion in solids, *Acta Mech.* **37**, 265-296 (1980).

16. E.C. Aifantis, Elementary physicochemical degradation processes, *Int. Symp. on Mech. Beh. of Str. Media*, Ottawa, Canada, Elsevier Sci. Publ. Co., 1981.

20

17. D.J. Unger and E.C. Aifantis, On the theory of stress-assisted diffusion II, *Acta Mech.* **47**, 117-151 (1983).

18. D.J. Unger, W.W. Gerberich and E.C. Aifantis, Further remarks on the implications of steady-state stress-assisted diffusion on environmental cracking, *Scripta Met.* **16**, 1059-1064 (1982) .

19. H. Chung, D.J. Unger D.D. McDonald and E.C. Aifantis, Steady and non-steady crack growth under environmental conditions, preprint.

20. D.J. Unger, *Analytical Fracture Mechanics*, Academic Press, London, England, 1995.

21. E.C. Aifantis, Recent results in the phenomenological theory of diffusion, T\&AM Report 430, UILU-ENG 78-6008, University of Illinois, Urbana Illinois (1978).

22. T. Vicsek, *Fractal Growth Phenomena*, 2nd edition, World Scientific, Singapore, 1992